4 1D FEL analysis

In this chapter we delve more deeply into the 1D theory of the FEL. The 1D picture is sufficient to understand how an FEL works, since the essential FEL physics is longitudinal in nature. A free-electron laser acts as a linear amplifier in the small signal regime, and we will find that it is most easily analyzed theoretically in the frequency representation. Hence, we begin this section by deriving the FEL equations in the frequency domain, including both the 1D wave equation and the Klimontovich equation describing the electron beam. We then apply these equations to the small-gain limit in Sec. 4.2, finding solutions that generalize those of Sec. 3.3. We then turn our attention to the high-gain FEL in Sec. 4.3, showing how the linearized FEL equations can be solved for arbitrary initial conditions using the Laplace transform. In particular, Sec. 4.3 covers self-amplified spontaneous emission (SASE) in some detail, because SASE provides the simplest way to produce intense x-rays. We derive the basic properties of SASE in the frequency domain, including its initialization from the fluctuations in the electron beam density (shot noise), its exponential gain, and its spectral properties. We then connect our analysis to the time domain picture via Fourier transfomation, which helps complete the characterization of SASE's fluctuation properties. The Chapter concludes with a discussion of how the FEL gain saturates in Sec. 4.4. We derive a quasilinear theory that describes the decrease in gain associated with an increase in electron beam energy spread, and show qualitatively how this is related to particle trapping. We also discuss tapering the undulator strength parameter after saturation to further extract radiation energy from the electron beam. Finally, we make a few comments on superradiance, focusing on the superradiant FEL solution associated with particle trapping that can support powers in excess of the usual FEL saturation power.

4.1 Coupled Maxwell-Klimontovich equations for the 1D FEL

The 1D FEL equations in the frequency domain can be used to obtain a clear understanding of various aspects of the SASE process, including the initial start-up from particle shot noise, the exponential gain, the development of longitudinal coherence, and the effect of the electron beam energy spread. They also qualitatively describes the full physics of x-ray FELs, since the effect of diffraction is

smaller for shorter wavelengths. Here, we first derive the spectral wave equation, and then turn to a frequency representation of the Klimontovich equation that describes the dynamics of the electron distribution function.

4.1.1 Wave equation in the frequency domain

In the previous Chapter we derived the wave equation (3.73) for the slowly varying complex amplitude $E(t;z)$. In order to obtain this equation, we averaged the Maxwell wave equation over time both to isolate the amplitude E and to properly define the slowly-varying current. Only after integrating over the time interval Δt did the slowly-varying current become apparent – prior to the averaging J_x contained an ill-defined sum of Dirac delta-functions. This time-domain approach is convenient for developing an understanding of the high-gain behavior and scalings, and is well-suited to time-dependent numerical simulation (e.g., the FEL codes GINGER or GENESIS). The approximation involving the Δt average becomes accurate in the exponential growth regime when the e-beam has developed significant bunching. On the other hand, the same average is not well-defined in the initial stage when the electron distribution is completely stochastic. For this reason the study of self-amplified spontaneous emission, which involves an intense signal growing from initially random noise, is more appropriately carried out in the frequency domain.

We introduce the slowly varying frequency domain amplitude $\tilde{E}_\nu$ via

$$E_x(z,t) = e^{ik_1(z-ct)} \int d\nu \; \tilde{E}_\nu(z) e^{i\Delta\nu k_1(z-ct)} + c.c., \tag{4.1}$$

where we recall that the normalized frequency difference $\Delta\nu \equiv (\nu - 1) \equiv (k - k_1)/k_1$ for the fundamental $h = 1$. This definition differs slightly from the conventions used in the chapter on spontaneous radiation, since the complex conjugate implies that (4.1) includes only positive frequencies; nevertheless, this is consistent with the power and flux definitions of Sec. 1.2.2, which count only positive frequencies as seen in Eq. (1.69). For FEL radiation, we expect $\tilde{E}_\nu$ to be localized about the resonant frequency with $\Delta\nu \ll 1$, so that the ν-integral extends only over a narrow range about $\nu = 1$. This restriction has the same physical significance as the Δ-slice averaging in the time domain.

We now proceed to derive the frequency-domain field equation in 1D by neglecting the transverse dependence in the paraxial wave equation (2.64) obtained when studying synchroton radiation. We proceed this way for several reasons: first, we want to emphasize the fact that the FEL is a natural extention of spontaneous undulator radiation once the self-consistent electron motion in the radiation field is included; second, our approach to undulator radiation also included emission at the odd harmonics, so that using our results from Sec. 2.4 will also yield the wave equation for higher FEL harmonics; third, our Δ-slice average somewhat complicates a direct Fourier transformation of the time-domain equation (3.76). Hence, we begin by re-writing the paraxial solution (2.64) with

two modifications to the source that we explain below:

$$\left[\frac{\partial}{\partial z}+\frac{ik}{2}\boldsymbol{\phi}^2\right]\tilde{\mathcal{E}}_\omega(\boldsymbol{\phi};z)=\sum_{h\ \text{odd}}\frac{eK[\text{JJ}]_h}{8\pi\epsilon_0\gamma_r c\lambda^2}\sum_{j=1}^{N_e}e^{-i\omega\theta_j(z)/\omega_1}e^{i\Delta\nu k_u z}\times\int d\boldsymbol{x}\ e^{-ik\boldsymbol{\phi}\cdot\boldsymbol{x}}\delta(\boldsymbol{x}-\boldsymbol{x}_j). \tag{4.2}$$

First and foremost, we have replaced the initial particle time coordinate with the dynamical phase via $t_j(0)\to\bar{t}_j(z)-(k_1+k_u)z/\omega_1=-\theta_j(z)/\omega_1$. This generalizes the source to include self-consistent particle motion in the ponderomotive potential.[1] Second, we have re-written the angular dependence of the current so that we can replace the point-like electron source with a constant charge density in the transverse plane by making the replacement $\delta(\boldsymbol{x}-\boldsymbol{x}_j)\to 1/(2\pi\sigma_x^2)$. Then, in the 1D limit we have

$$\int d\boldsymbol{x}\ e^{-ik\boldsymbol{\phi}\cdot\boldsymbol{x}}\delta(\boldsymbol{x}-\boldsymbol{x}_j)\to\int d\boldsymbol{x}\ \frac{e^{-ik\boldsymbol{\phi}\cdot\boldsymbol{x}}}{2\pi\sigma_x^2}=\frac{\lambda^2}{2\pi\sigma_x^2}\delta(\boldsymbol{\phi}), \tag{4.3}$$

and the source is directed entirely in the forward direction.

The 1D limit is completed by defining the 1D electric field via

$$\tilde{\mathcal{E}}_\omega(\boldsymbol{\phi};z)=\frac{\tilde{E}_\nu(z)}{ck_1}\delta(\boldsymbol{\phi}). \tag{4.4}$$

The factor $1/ck_1$ accounts for the fact that the Fourier transform (4.1) is defined with respect to the scaled frequency ν rather than ω; the $\delta(\boldsymbol{\phi})$ enforces the field to be in the forward direction only, which also implies that in the spatial representation the electric field is independent of $\boldsymbol{x}$. Inserting the field (4.4) into (4.2) and integrating over angle yields the 1D field equation in the frequency domain

$$\frac{\partial}{\partial z}\tilde{E}_\nu=-\frac{ek_1K[\text{JJ}]_h}{8\pi\sigma_x^2\epsilon_0\gamma_r}e^{i\Delta\nu k_u z}\frac{1}{2\pi}\sum_{j=1}^{N_e}e^{-i\nu\theta_j(z)}. \tag{4.5}$$

We recall that the phase $\theta_j(z)$ is the position of the j^{th} electron relative to the bunch center in units of $\lambda_1/2\pi$, and λ_1 is the fundamental wavelength of the undulator radiation.

Finally, we clean up the source current in the wave equation (4.5) by defining the phase-shifted electric field amplitude

$$E_\nu(z)=e^{-i\Delta\nu z}\tilde{E}_\nu(z). \tag{4.6}$$

Note that this phase shift must be retained even though $\Delta\nu\sim\rho$, since we also have $k_u z\sim 1/\rho$. The field equation for $E_\nu(z)$ is then

$$\left(\frac{\partial}{\partial z}+i\Delta\nu k_u\right)E_\nu(z)=-\frac{ek_1K[\text{JJ}]_h}{8\pi\sigma_x^2\epsilon_0\gamma_r}\frac{1}{2\pi}\sum_{j=1}^{N_e}e^{-i\nu\theta_j(z)}. \tag{4.7}$$

[1] Previously we calculated the spontaneous undulator radiation assuming that the electrons move with the average longitudinal velocity $\bar{v}_z=\omega_1/(k_1+k_u)$, in which case $\theta_j(z)=-\omega_1 t_j(0)$.

Although this equation looks very similar to the time domain Eq. (3.76), the frequency domain wave equation (4.5) differs in the following ways in that the driving current is a sum over all electrons in the bunch, and the particle phase factor is $e^{-i\nu\theta}$ instead of $e^{-i\theta}$.

4.1.2 Particle dynamics: Klimontovich equation

In our previous analysis we have described the electron motion in an FEL using single particle (Newton's) equations, from which we found an approximate collective description. An alternate approach that retains all the generality of the single particle equations while treating the electron beam as a single entity employs a distribution function on phase space. It turns out that this approach is also naturally suited for the frequency representation.

To retain the discrete nature of the electrons, we describe the electron beam using the Klimontovich distribution function in the longitudinal phase space spanned by (θ, η),

$$F(\theta, \eta; z) = \frac{k_1}{I/ec} \sum_{j=1}^{N_e} \delta[\theta - \theta_j(z)]\delta[\eta - \eta_j(z)]. \tag{4.8}$$

Here I/ec is the line density, and F is comprised of sum over all N_e particles in the beam, with each particle contributing a delta function centered about its coordinates in phase space.

The distribution function can be separated into the smooth background V and the rest that contains the shot noise and the perturbation due to the FEL interaction δF. We write this division as

$$F(\theta, \eta; z) = V(\eta) + \delta F(\theta, \eta; z), \tag{4.9}$$

in which we assume that the smooth background distribution depends only on the energy η but not on the phase θ. This corresponds to a uniform bunch model which is approximately valid for a bunch that is much longer than the slippage distance over one gain length, $\lambda_1/4\pi\rho$. Furthermore, we have taken V to be independent of z, an assumption that applies before nonlinear saturation. Its normalization is chosen such that $\int d\eta\, V(\eta) = 1$.

The frequency representation of the Klimontovich distribution function $F(\theta, \eta; z)$ is given by

$$F_\nu(\eta; z) = \frac{1}{2\pi} \int d\theta\, e^{-i\nu\theta} F(\theta, \eta; z) = \frac{1}{N_\lambda} \sum_{j=1}^{N_e} e^{-i\nu\theta_j(z)} \delta[\eta - \eta_j(z)], \tag{4.10}$$

where N_λ is the number of electrons in one radiation wavelength λ_1. Conservative, Hamiltonian dynamics dictates that the distribution function is conserved along single particle orbits, so that F satisfies the continuity equation

$$\frac{d}{dz} F(\theta, \eta; z) = \frac{\partial F}{\partial z} + \frac{d\theta}{dz}\frac{\partial F}{\partial \theta} + \frac{d\eta}{dz}\frac{\partial F}{\partial \eta} = 0. \tag{4.11}$$

The phase equation $d\theta_j/dz$ is the same as was derived previously; the energy equation in terms of $E_\nu(z)$ can be found by comparing the definitions (3.60) and (4.1), from which we find that

$$e^{i\theta_j}E(z,\theta_j) = e^{i\theta_j}\int d\nu\ \tilde{E}_\nu(z)e^{i\Delta\nu k_1(z-ct_j)} = e^{i\theta_j}\int d\nu\ \tilde{E}_\nu(z)e^{-i\Delta\nu z}e^{i\Delta\nu\theta_j}$$
$$= \int d\nu\ E_\nu(z)e^{i\nu\theta_j}. \tag{4.12}$$

If we include the force due to all odd radiation harmonics, the Vlasov equation (4.11) becomes

$$\left[\frac{\partial}{\partial z} + 2k_u\eta\frac{\partial}{\partial\theta}\right]\delta F = -\sum_{h\ \text{odd}}\chi_h\left[\int d\nu\ E_\nu(z)e^{i\nu\theta} + c.c.\right]\frac{\partial}{\partial\eta}(V+\delta F), \tag{4.13}$$

where we have defined the harmonic coupling $\chi_h = eK[\mathrm{JJ}]_h/(2\gamma_r^2 mc^2)$ and assumed that the radiation frequency is narrowly centered about each harmonic, so that $\nu \approx h$ for $h = 1, 3, \ldots$.

In what follows we will further assume that only one radiation harmonic contributes to the sum, and treat δF and E_ν as first order quantities. In this small-signal limit we may drop the term $\sim \delta F$ from the right-hand-side of (4.13), leaving only the (zeroth order) smooth background $V(\eta)$. Fourier transforming the result gives the linearized continuity equation in the frequency representation as

$$\left[\frac{\partial}{\partial z} + 2i\nu k_u\eta\right]F_\nu(\eta;z) = -\chi_h\frac{dV}{d\eta}E_\nu(z). \tag{4.14}$$

The 1D Maxwell-Klimontovich equations for the FEL are then completed by using the definition (4.10) to express the source term of the wave equation (4.7) in terms of F_ν; we get

$$\left(\frac{\partial}{\partial z} + i\Delta\nu k_u\right)E_\nu(z) = -\kappa_h n_e\int d\eta\ F_\nu(\eta;z), \tag{4.15}$$

where the harmonic coupling

$$\kappa_h \equiv \frac{eK[\mathrm{JJ}]_h}{4\epsilon_0\gamma_r}. \tag{4.16}$$

It is easy to show that (4.15) with $h = 1$ is related to the field equation (3.76) by the Fourier transform defined in (4.1). We recall that the electron volume density

$$n_e = \frac{I}{ec(2\pi\sigma_x^2)}, \tag{4.17}$$

and that in the 1D limit the cross sectional area $2\pi\sigma_x^2$ is assumed to be large. For the FEL this implies that the electron beam width should be much larger than the natural FEL mode size, with $\sigma_x^2 \gg \lambda_1\lambda_u/(4\pi^2\rho)$.

We pause to make a brief comment on our assumption that only one FEL

harmonic contributes to the equation (4.14). In the low-gain case this means that we consider the amplification of a nearly monochromatic field whose frequency is centered at $h\omega_1$ with h odd and positive. This situation is particularly relevant to an FEL oscillator designed to amplify one frequency over many passes through the undulator. On the other hand, our high-gain analysis will assume that the FEL operates at the fundamental frequency because this gives the largest gain, so that high-gain devices typically operate with $h = 1$. While the generation of harmonic radiation is possible with a high-gain device, this typically involves nonlinear processes that we will discuss in Chap. 6.

4.2 Pertubative solution for small FEL gain

We have shown that in the linear regime the FEL is governed by the coupled differential equations (4.15) and (4.14). It is easy to see that these are equivalent to the integral equations

$$E_\nu(z) = e^{-i\Delta\nu k_u z}\left[E_\nu(0) - \kappa_h n_e \int_0^z dz'\, e^{i\Delta\nu k_u z'} \int d\eta\, F_\nu(\eta; z')\right] \tag{4.18}$$

$$F_\nu(\eta; z) = e^{-2i\nu k_u \eta z}\left[F_\nu(\eta; 0) - \chi_h \int_0^z dz'\, e^{2i\nu k_u \eta z'} \frac{dV}{d\eta} E_\nu(z')\right]. \tag{4.19}$$

Combining these two, we find that the electric field satisfies

$$\begin{aligned} E_\nu(z) = e^{-i\Delta\nu k_u z}\Bigg[&E_\nu(0) - \kappa_h n_e \int_0^z dz' \int d\eta\, e^{i(\Delta\nu - 2\nu\eta)k_u z'} F_\nu(\eta; 0) \\ &+ \chi_h \kappa_h n_e \int_0^z dz'\, e^{i(\Delta\nu - 2\nu\eta)k_u z'} \int_0^{z'} dz''\, e^{2i\nu k_u \eta z''} \frac{dV}{d\eta} E_\nu(z'')\Bigg]. \end{aligned} \tag{4.20}$$

The first term on the right-hand side is the input coherent radiation that propagates unaltered to the point z, while the second term is the spontaneous undulator radiation; we abbreviate the latter as

$$E_\nu^{\mathrm{SR}}(z) \equiv -\kappa_h n_e e^{-i\Delta\nu k_u z} \int_0^z dz' \int d\eta\, e^{i(\Delta\nu - 2\nu\eta)k_u z'} F_\nu(\eta; 0). \tag{4.21}$$

The third term in Eq. (4.20) represents the effects of the interaction between the electron beam and the radiation field.

As it stands, (4.20) clearly separates the initial, spontaneous, and amplified parts of the radiation field, but is in general more difficult to solve then (4.15) and (4.14). If the interaction is weak, however, we may replace $E_\nu(z'')$ with the unperturbed field $e^{-i\Delta\nu k_u z''} E_\nu(0)$ in the interaction term. In this case we have

a closed-form solution that we can write as

$$E_\nu(z) = E_\nu^{\rm Coh}(z) + E_\nu^{\rm SR}(z), \tag{4.22}$$

where in the weak-interaction (low-gain) approximation the coherent part of the field is

$$E_\nu^{\rm Coh}(z) = e^{-i\Delta\nu k_u z} E_\nu(0) \times \left[1 + \chi_h \kappa_h n_e \int d\eta \int_0^z dz' \int_0^{z'} dz''\, e^{i(\Delta\nu - 2\nu\eta)k_u(z'-z'')} \frac{dV}{d\eta}\right]. \tag{4.23}$$

The integrals over z' and z'' are straightforward, and at the end of the undulator the coherent field can be cast in the form

$$E_\nu^{\rm Coh}(L_u) = \left\{1 + \frac{j_{C,h}}{8} \int d\eta\, V(\eta)[g(x_{\nu,\eta}) + ip(x_{\nu,\eta})]\right\} e^{-2\pi i \Delta\nu N_u} E_\nu(0). \tag{4.24}$$

The compact solution (4.24) obtains after integrating over η by parts and introducing additional short-hand notation with the constant $j_{C,h}$ and the functions p and g. We have defined $g(x)$ to be the same as the gain function introduced when we first discussed low-gain FEL physics in Sec. 3.3.1, while we will find that the function $p(x)$ is related to the accompanying phase change of $E_\nu(z)$. Explicitly, these functions are

$$g(x) = -\frac{d}{dx}\left(\frac{\sin x}{x}\right)^2 \qquad p(x) = \frac{d}{dx}\left(\frac{2x - \sin x}{2x^2}\right). \tag{4.25}$$

We assume that the frequency is near an odd harmonic, $\nu = h + \Delta\nu$ with h odd and $\Delta\nu \ll 1$, in which case g and p are functions of the argument

$$x_{\nu,\eta} = 2\pi N_u(h\eta - \Delta\nu/2). \tag{4.26}$$

Finally, the dimensionless constant $j_{C,h}$ was introduced by Colson in his low gain FEL analysis [1], and defined to be

$$j_{C,h} \equiv 4h\chi_h\kappa_h n_e k_u L_u^3 = 4\pi^2 h \frac{e^2 n_e}{4\pi\epsilon_0} \frac{K^2 [\mathrm{JJ}]_h^2}{\gamma^3 mc^2} N_u L_u^2 \tag{4.27}$$

$$= 2h(4\pi\rho N_u)^3 \frac{[\mathrm{JJ}]_h^2}{[\mathrm{JJ}]^2}. \tag{4.28}$$

The second line shows the relationship between $j_{C,h}$ and the dimensionless Pierce parameter ρ that we introduced in Sec. 3.4.3. Since $j_{C,h}$ is proportional to the gain when the gain is small, in this limit we also find that $G \propto (\rho N_u)^3$. Again, the low-gain solution (4.24) is valid if $j_{C,h} \ll 1$, which is equivalent to requiring that the undulator length is less then the ideal 1D FEL gain length, $L_u/L_{G0} = 4\pi\sqrt{3}\rho N_u < 1$. This requirement can be relaxed somewhat if the gain is reduced by the energy spread of the electron beam.

To investigate the effects of the electron beam energy spread, we consider the

case where the electrons' energy distribution is Gaussian about η_0:

$$V(\eta) = \frac{1}{\sqrt{2\pi}\sigma_\eta} e^{-(\eta-\eta_0)^2/2\sigma_\eta^2}. \tag{4.29}$$

We then write the amplitude formula (4.24) as

$$E_\nu^{\rm Coh}(L_u) = \left\{1 + \frac{j_{C,h}}{8}\left[\bar{g}(x_0) + i\bar{p}(x_0)\right]\right\} e^{-2\pi i \Delta\nu N_u} E_\nu(0). \tag{4.30}$$

Here, we have defined the integrations

$$\bar{g}(x_0) \equiv \int dx' \, \frac{e^{-x'^2/2(2\pi N_u h\sigma_\eta)^2}}{\sqrt{2\pi}(2\pi N_u h\sigma_\eta)} g(x_0 - x'), \tag{4.31}$$

$$\bar{p}(x_0) \equiv \int dx' \, \frac{e^{-x'^2/2(2\pi N_u h\sigma_\eta)^2}}{\sqrt{2\pi}(2\pi N_u h\sigma_\eta)} p(x_0 - x'), \tag{4.32}$$

with $x_0 \equiv 2\pi N_u(h\eta_0 - \Delta\nu/2)$.

Now, we can easily calculate the gain by considering the radiation energy density $u \propto |E_\nu|^2$. We have

$$G = \frac{u(L_u) - u(0)}{u(0)} \approx \frac{j_{C,h}}{4}\bar{g}(x_0) \tag{4.33}$$

to first order in $j_{C,h}$. This expression generalizes the gain formula (3.47) to include e-beam energy spread; in the limit $\sigma_\eta \ll 1/(2\pi N_u h)$ we have $\bar{g}(x_0) \to g(x_0)$ and (4.33) reproduces (3.47). In other words, the electron beam energy spread can be neglected if its rms width is much less than that of the spontaneous radiation at the FEL harmonic of interest. On the other hand, if the energy spread $\sigma_\eta \gtrsim 1/(2\pi N_u h)$ then we must account for the fact that electrons with different energies satisfy the FEL resonance condition at different radiation wavelengths. The resulting interference tends to reduce the FEL gain, and this physics is captured mathematically by the convolution (4.31).

There is another convenient way to write $\bar{g}(x_0)$ if the energy distribution is given by the Gaussian (4.29). This expression follows if we defer integrating over the undulator length in Eq. (4.23), and instead integrate over η. Changing variables to $z = z'/L_u - 1/2$ and $s = z''/L_u - 1/2$ we find that

$$G = -\frac{j_{C,h}}{2} \int_{-1/2}^{1/2} dz \int_{-1/2}^{1/2} ds \, (z-s)\sin[2x_0(z-s)] e^{-2[2\pi N_u(z-s)\sigma_\eta]^2}. \tag{4.34}$$

In addition to energy exchange, the amplitude equation has an imaginary part proportional to $p(x)$. This term in Eq. (4.30) leads to a phase change of the field that accompanies FEL gain. Figure 4.1(a) plots the functions $\bar{g}(x)$ and $\bar{p}(x)$ as a function of the detuning $x_0 = 2\pi N_u(h\eta_0 - \Delta\nu/2)$ when the energy spread $\sigma_\eta = 0.5(2\pi N_u h)$. The functional form of g is very similar to the zero energy spread case shown previously in Fig. 3.6, although the peak value has decreased from 0.54 to about 0.46. The value of p at the detuning that maximizes the gain

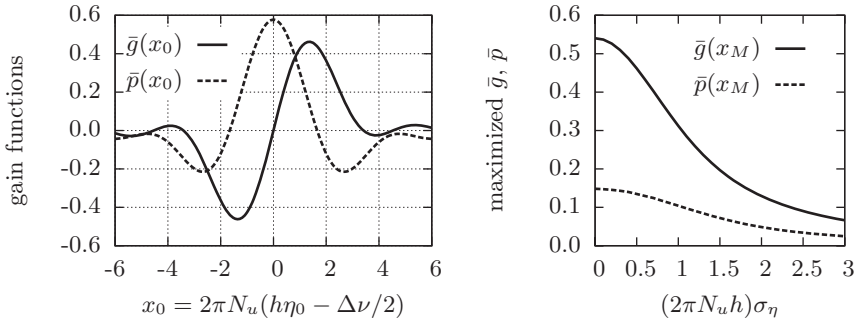

Figure 4.1 (a) Low-gain functions when the energy spread $(2\pi N_u h)\sigma_\eta = 0.5$. The amplitude gain $\bar{g}$ is very similar to its cold counterpart, while the phase change $\bar{p}$ is small at maximum gain. (b) Energy spread dependence of the low-gain functions at the detuning x_M that gives maximal gain.

is small, about 0.13. Therefore, the phase change during FEL amplification is also relatively small.

We are usually free to set the detuning x to maximize the gain, by either choosing the energy or frequency offset (in fact, the FEL itself may pick out the x of maximum gain). In Fig. 4.1(b) we plot $\bar{g}$ and $\bar{p}$ at the detuning x_M that maximizes the gain. We see that the phase change $\bar{p}$ is between one-quarter and two-fifths of $\bar{g}$, and is therefore typically rather small.

Furthermore, we see that the gain is not significantly affected by the energy spread provided $(2\pi N_u h)\sigma_\eta \lesssim 0.5$, after which $\bar{g}$ drops quite rapidly. This shows that the FEL gain at higher harmonics is more sensitive to energy spread, which can be attributed to the fact that the normalized undulator radiation bandwidth $\sim 1/hN_u$. On the other hand, the FEL gain for a fixed e-beam energy, undulator period, and undulator length also scales with the constant $j_{C,h} \propto hK^2[\mathrm{JJ}]_h^2$. Hence, under these restrictions one may find that the gain at a certain target wavelength is maximized by operating at a higher FEL harmonic, because in this case $j_{C,h}$ increases as both h and K increase. This will be true provided the energy spread is sufficiently small, $\sigma_\eta \lesssim 1/(4\pi N_u h)$. Such constraints on e-beam energy or undulator length may be imposed by cost and/or size limits of the FEL accelerator facility.

4.3 Solution via Laplace transformation for arbitrary FEL gain

We employed two different perturbation expansions in Sec. 3.2 and in Sec. 4.2 to solve the FEL equations in the low-gain limit. Here, we develop the full solution to the linearized 1D FEL equations that will generalize the collective variable approach of Sec. 3.4.4. We assume emission at the fundamental dominates the

dynamics ($\nu \approx 1$), so that the coupled FEL system is described by

$$\left(\frac{\partial}{\partial z} + i\Delta\nu k_u\right) E_\nu(z) = -\kappa_1 n_e \int d\eta\, F_\nu(\eta; z), \tag{4.35}$$

$$\left[\frac{\partial}{\partial z} + 2ik_u\eta\right] F_\nu(\eta; z) = -\chi_1 \frac{dV}{d\eta} E_\nu(z). \tag{4.36}$$

The initial value problem of the coupled Eqs. (4.35) and (4.36) can be solved by introducing the Laplace transform [2, 3]:

$$\begin{bmatrix} E_{\nu,\mu} \\ F_{\nu,\mu} \end{bmatrix} = \int_0^\infty dz\, e^{i\mu 2\rho k_u z} \begin{bmatrix} E_\nu(z) \\ F_\nu(z) \end{bmatrix}. \tag{4.37}$$

We emphasize that $\nu \approx 1$ represents the frequency that is the Fourier conjugate to the temporal phase θ, while μ gives complex growth as the fields propagate in z. Taking the Laplace transform of the particle and radiation equations lead to the algebraic linear system

$$-2i\mu\rho k_u E_{\nu,\mu} + i\Delta\nu k_u E_{\nu,\mu} = -\kappa_1 n_e \int d\eta\, F_{\nu,\mu}(\eta) + E_\nu(0) \tag{4.38}$$

$$-2i\mu\rho k_u F_{\nu,\mu}(\eta) + 2ik_u\eta F_{\nu,\mu}(\eta) = -\chi_1 E_{\nu,\mu} \frac{dV}{d\eta} + F_\nu(\eta; 0), \tag{4.39}$$

where $E_\nu(0)$ and $F_\nu(\eta; 0)$ are the ν^{th} component of the initial radiation field and the initial beam distribution, respectively. Equations (4.38)-(4.39) can be easily solved for $E_{\nu,\mu}$, and the inverse Laplace transformation yields

$$E_\nu(z) = \oint \frac{d\mu}{2\pi i} \frac{e^{-i\mu 2\rho k_u z}}{D(\mu)} \left[E_\nu(0) + \frac{i\kappa_1 n_e}{2\rho k_u N_\lambda} \sum_{j=1}^{N_e} \frac{e^{-i\nu\theta_j(0)}}{\eta_j(0)/\rho - \mu}\right], \tag{4.40}$$

where we have used the definition of F_ν Eq. (4.10), and have defined the dispersion function

$$D(\mu) \equiv \mu - \frac{\Delta\nu}{2\rho} - \int d\eta\, \frac{V(\eta)}{(\eta/\rho - \mu)^2}. \tag{4.41}$$

Note that the integration contour in the complex μ plane must be below all singularities/poles of (4.40), so that when $z < 0$ and the contour can be closed at $\Im(\mu) \to -\infty$, it encloses no poles and $E_\nu(z < 0) = 0$.

The first term of Eq. (4.40) describes the process of coherent amplification of $E_\nu(0)$, while the second term containing the particle phases $e^{-i\nu\theta_j}$ describes FEL radiation initiated by the electron beam; assuming that the beam is not initially microbunched these phases are random and this term describes the process of self-amplified spontaneous emission.

When $z > 0$ the contour integral of Eq. (4.40) encloses all the singularities in the complex μ plane. There are many singularities of kinematic origin, which give the free-streaming solutions for which $\mu = \eta_j(0)/\rho$; however, these vary for each particle according to the initial energy, and we will find that summing over these contributions yield the usual spontaneous emission. Thus, the evolution in

a free-electron laser is largely dictated by the poles of $1/D$, which are given by the roots of the dispersion relation:

$$D(\mu) = \mu - \frac{\Delta\nu}{2\rho} - \int d\eta \, \frac{V(\eta)}{(\eta/\rho - \mu)^2} = 0. \tag{4.42}$$

Solutions to $D(\mu) = 0$ for which μ has a positive imaginary part give rise to an exponentially growing electric field amplitude. For e-beams with vanishing energy spread $V(\eta) = \delta(\eta)$, this dispersion relation become $\mu^2(\mu - \Delta\nu/2\rho) = 1$, which in turn reduces to the cubic equation (3.97) when $\Delta\nu = 0$.

Having found the field amplitude, we can compute the power spectral density with some slight adjustments to the formula (1.70). Using the fact that $E_\omega = E_\nu/\omega_1$ and integrating over the area $2\pi\sigma_x^2$, we find that

$$\frac{dP}{d\omega} = \frac{\epsilon_0}{\pi c} \frac{2\pi\sigma_x^2\lambda_1^2}{T} \left\langle |E_\nu(z)|^2 \right\rangle. \tag{4.43}$$

Here T is the duration of the electron pulse, and $\langle\cdot\rangle$ denotes an ensemble average over the microscopic electron distribution. When calculating $\left\langle \, |E_\nu(z)|^2 \, \right\rangle$ for the SASE term we will use the manipulation

$$\begin{aligned} \left\langle \sum_{j,\ell} e^{-i\nu(\theta_j - \theta_\ell)} G(\eta_j, \eta_\ell) \right\rangle &= \left\langle \sum_j G(\eta_j, \eta_j) \right\rangle + \left\langle \sum_{j \neq \ell} e^{-i\nu(\theta_j - \theta_\ell)} G(\eta_j, \eta_\ell) \right\rangle \\ &\approx N_e \int d\eta \, V(\eta) G(\eta, \eta), \end{aligned} \tag{4.44}$$

where the θ_j's are the initial phases, and we drop the sum with $j \neq \ell$ under the assumption that the initial phases are completely random with no correlation. For simplicity, we use the shorthanded notation $\theta_j = \theta_j(0)$ and $\eta_j = \eta_j(0)$ from now on.

4.3.1 Spontaneous radiation and the low-gain limit

The system dynamics are largely governed by the dispersion function $D(\mu)$ of Eq. (4.41). The FEL interaction itself is contained in the third term here, and involves an integral over η of the distribution function V. We can connect the present analysis with our calculation of the spontaneous undulator radiation and the low-gain FEL by assuming this interaction to be weak. Thus, we expand $1/D$ from the integral solution (4.40) as follows:

$$\frac{1}{D(\mu)} = \frac{1}{\mu - \Delta\nu/(2\rho)} + \frac{1}{(\mu - \Delta\nu/(2\rho))^2} \int d\eta \, \frac{V(\eta)}{(\eta/\rho - \mu)^2} + \dots . \tag{4.45}$$

This expansion is valid mathematically in the limit of vanishing ρ, and hence we also have $\eta/\rho \to \infty$.

We compute the spontaneous radiation amplitude by keeping only the first term in the expansion and applying the residue theorem of contour integration.

Then, we get

$$E_\nu(z) = -\frac{i\kappa_1 n_e}{2\rho k_u N_\lambda} \sum_{j=1}^{N_e} e^{-i\nu\theta_j} \frac{e^{-i\Delta\nu k_u z} - e^{-2i\eta_j k_u z}}{\eta_j/\rho - \Delta\nu/2\rho}, \tag{4.46}$$

which is easy to show is the equal to the spontaneous radiation amplitude obtained in the perturbation expnasion (4.20). To find the power spectral density, we insert $E_\nu(z)$ into Eq. (4.43) and evaluate the ensemble average with the help of Eq. (4.44):

$$\begin{aligned} \left.\frac{dP}{d\omega}\right|_{1D} &= \left(\frac{\lambda_1^2}{2\pi\sigma_x^2}\right) \frac{I}{I_A} \left(\frac{K[\mathrm{JJ}]}{1+K^2/2}\right)^2 \frac{\gamma^2 mc^2 z^2}{\lambda_u^2} \\ &\quad \times \int d\eta\, V(\eta) \left\{\frac{\sin[k_u z(\eta - \Delta\nu/2)]}{k_u z(\eta - \Delta\nu/2)}\right\}^2. \end{aligned} \tag{4.47}$$

The quantity $\lambda_1^2/(2\pi\sigma_x^2)$ can be interpreted as the characteristic diffraction angular spread from a source of size $2\pi\sigma_x^2$: $\Delta\phi_x\Delta\phi_y \sim \lambda_1^2/(2\pi\sigma_x^2)$. In the 1D limit this tends to zero, and we identify

$$\delta(\boldsymbol{\phi})\big|_{\phi=0} = \frac{2\pi\sigma_x^2}{\lambda_1^2} \tag{4.48}$$

to relate our 1D result to the spectral-angular distribution of the radiation power in the forward direction via

$$\left.\frac{dP}{d\omega}\right|_{1D} \frac{2\pi\sigma_x^2}{\lambda_1^2} = \frac{dP}{d\omega}\delta(\boldsymbol{\phi})\big|_{\phi=0} = \left.\frac{dP}{d\omega d\boldsymbol{\phi}}\right|_{\phi=0}. \tag{4.49}$$

Equations (4.47) and (4.49) give the well-known formula for undulator radiation, which we derived previously as (2.97).

It is left as an exercise to show that the low-gain FEL theory can be reproduced by keeping the second term of the expansion Eq. (4.45) into Eq. (4.40).

4.3.2 Exponential growth regime

In general, the dispersion relation may have a root with positive imaginary part that in turn gives rise to an exponentially growing field amplitude. In keeping with previous notation, we denote this root as μ_3, so that $\Im(\mu_3) > 0$. As $\rho k_u z$ becomes larger than unity the growing solution associated with μ_3 tends to dominate the field dynamics, in which case the field is well-described by a single mode. Applying the residue theorem and keeping only the term associated with the growing root μ_3 gives

$$E_\nu(z) = \frac{e^{-2i\rho\mu_3 k_u z}}{D'(\mu_3)} \left[E_\nu(0) + \frac{i\kappa_1 n_e}{2\rho k_u N_\lambda} \sum_{j=1}^{N_e} \frac{e^{-i\nu\theta_j}}{\eta_j/\rho - \mu_3}\right], \tag{4.50}$$

where

$$D'(\mu) = \frac{dD}{d\mu} = 1 - 2\int d\eta\, \frac{V(\eta)}{(\eta/\rho - \mu)^3}. \tag{4.51}$$

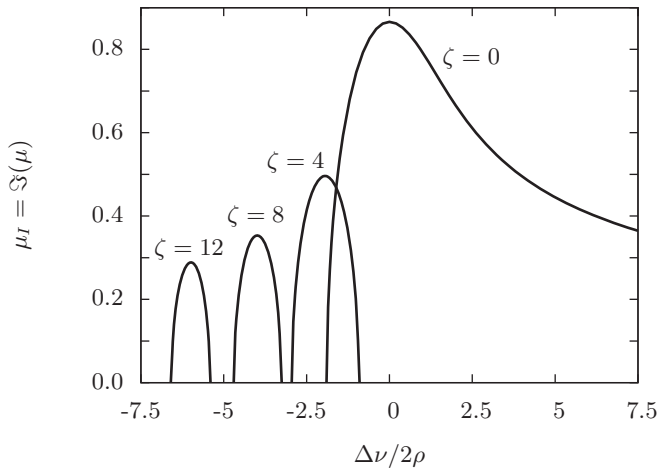

Figure 4.2 The growth rate μ_I as a function of the scaled detuning $\Delta\nu/2\rho$ for a flattop energy distribution with the full width $\Delta\eta = \zeta\rho$, for various values of ζ. Adapted from Ref. [2].

The corresponding electron distribution function, which can be obtained from Eq.(4.39), is

$$F_{\nu,\mu}(\eta) = \frac{i\chi_1}{2k_u}\frac{dV/d\eta}{(\nu\eta - \mu\rho)}E_{\nu,\mu}. \tag{4.52}$$

The power spectral density of the radiation in the exponential growth regime, which is computed by inserting Eq. (4.50) into Eq. (4.43), can be written as [2]

$$\frac{dP}{d\omega} = e^{4\mu_I\rho k_u z} g_A \left(\left.\frac{dP}{d\omega}\right|_0 + g_S \frac{\rho\,\gamma_r mc^2}{2\pi} \right), \tag{4.53}$$

where we write the imaginary part $\Im(\mu_3) \equiv \mu_I$, and the initial field and e-beam conditions are given by

$$\left.\frac{dP}{d\omega}\right|_0 \equiv \text{input power spectrum}, \tag{4.54}$$

$$g_A \equiv \frac{1}{|D'(\mu)|^2}, \tag{4.55}$$

$$g_S \equiv \int d\eta\, \frac{V(\eta)}{|\eta/\rho - \mu|^2}. \tag{4.56}$$

The quantities μ_I, g_A and g_S are all functions of the detuning $\Delta\nu$ and the electron beam energy distribution. g_A is a measure of how the initial radiation power and shot noise seed the interaction, while g_S quantifies the relative increase in shot noise seeding as the beam energy spread increases; we will discuss these coupling parameters further near the end of this section. The growth rate μ_I is a very important FEL figure of merit, as it sets the required undulator length

to reach saturation. As a simple example, Fig. 4.2 plots the growth rate μ_I as a function of $\Delta\nu/2\rho = \Delta\omega/(2\rho\omega_1)$ for various cases of the energy spread, assuming that the beam energy distribution is a flattop of full width $\Delta\eta = \rho\zeta$ [i.e., $V(\eta) = 1/\rho\zeta$ if $|\eta| \leq \rho\zeta/2$ and $V(\eta) = 0$ otherwise]. For this distribution, evaluating the integral in the dispersion relation (4.41) leads to

$$\left(\mu - \frac{\Delta\nu}{2\rho}\right)\left(\mu^2 - \frac{\zeta^2}{4}\right) = 1, \tag{4.57}$$

and the roots have closed form expressions. It turns out that this dispersion relation has the same functional form as that obtained including the quantum effects of recoil, and in Appendix C.1 we write the general solution to the initial value problem for the field, bunching, and collective momentum if μ obeys (4.57). Here, we focus on the growth rate; Figure 4.2 indicates that μ has a positive imaginary part over a frequency width characterized by the high-gain FEL bandwidth $\Delta\nu \sim \rho$. Additionally, the peak growth rate is a decreasing function of the energy width of the distribution function.

For a given electron beam energy spread, it is clearly interesting to compute the maximum value of μ_I, which we take to occur at a frequency detuning $\Delta\nu_m$: $\max_{\Delta\nu} \mu_I(\nu) = \mu_{Im}$ at $\Delta\nu = \Delta\nu_m$. The growth rate at frequencies near its maximum can be approximately determined by expanding μ_I as a Taylor series in $\Delta\nu$:

$$\mu_I(\Delta\nu) = \mu_{Im} - \mu_{I2}(\Delta\nu - \Delta\nu_m)^2 + \dots . \tag{4.58}$$

Thus, by approximating the growth rate as a quadratic function of the frequency difference about its maximum, we may write the exponential gain function as

$$e^{4\mu_I\rho k_u z} \approx e^{z/L_G} \exp\left[-\frac{1}{2}\left(\frac{\omega - \omega_m}{\omega_m\sigma_\nu}\right)^2\right] \tag{4.59}$$

where

$$4\mu_{Im}\rho k_u z \equiv \frac{z}{L_G} \qquad \omega_m \equiv \omega_1(1 + \Delta\nu_m) \qquad \sigma_\nu^2 \equiv \frac{1}{8\mu_{I2}\rho k_u z}. \tag{4.60}$$

Here, we have defined $L_G = (4\mu_{Im}\rho k_u)^{-1}$ to be the power gain length, while $\sigma_\nu \propto (\rho k_u z)^{-1/2}$ is the rms relative bandwidth of the FEL. Equation (4.59) approximates the frequency dependence of the FEL gain by a Gaussian function. This gain profile describes both the gain curve for coherent amplification of the initial spectral power $dP/d\omega|_0$, and the ensemble averaged spectral profile for the SASE term, since the beam shot noise acts as a white-noise (frequency-independent) seed as shown by Eq. (4.53). Note the phrase "ensemble averaged": we will subsequently show that SASE behaves like the chaotic light described in Sec. 1.2.5, so that any particular instance will be comprised of many longitudinal modes that appear as "spikes" in the single-shot temporal and spectral power profiles.

Now, we apply the Gaussian approximation (4.59) with the definitions (4.60)

to express the FEL power spectral density (4.53) as

$$\frac{dP}{d\omega} = g_A e^{z/L_G} \exp\left[-\frac{(\omega-\omega_m)^2}{2(\omega_m\sigma_\nu)^2}\right]\left(\left.\frac{dP}{d\omega}\right|_0 + g_S\frac{\rho\gamma_r mc^2}{2\pi}\right). \tag{4.61}$$

Equation (4.61), which is valid in the exponential growth regime $2\rho k_u z \gg 1$, shows how the power grows along the undulator.

For the special case of vanishing energy spread, the various parameters characterizing the 1D FEL have closed form solutions [2, 3]. From (4.41), the dispersion relation for a cold beam is

$$D(\mu) = \mu - \frac{\Delta\nu}{2\rho} - \frac{1}{\mu^2} = 0, \tag{4.62}$$

and the maximal growth rate is at zero detuning $\Delta\nu = 0$. It is then straightforward to show that

$$g_A = \frac{1}{9}, \qquad g_S = 1, \tag{4.63}$$

$$L_G = L_{G0} = \frac{\lambda_u}{4\pi\sqrt{3}\rho}, \qquad \mu_{Im} = \frac{\sqrt{3}}{2}. \tag{4.64}$$

These results are the same as what was predicted by the collective variable model. In addition, we can find the approximate dependence of the growth rate μ on frequency difference $\Delta\nu$ by expanding

$$\mu(\Delta\nu) \approx \mu(0) + \mu_1\Delta\nu + \mu_2\left(\Delta\nu\right)^2 \tag{4.65}$$

with $\mu(0) = (i\sqrt{3}-1)/2$ and assuming that $\Delta\nu/\rho \ll 1$. In this case, we solve (4.62) order by order in $\Delta\nu/\rho$, finding that

$$\mu \approx -\frac{1}{2}\left[1 - \frac{\Delta\nu}{3\rho} + \frac{(\Delta\nu)^2}{36\rho^2}\right] + i\frac{\sqrt{3}}{2}\left[1 - \frac{(\Delta\nu)^2}{36\rho^2}\right]. \tag{4.66}$$

Hence, $\mu_{I2} = \sqrt{3}/72\rho^2$, and the rms bandwidth for a beam with vanishing energy spread is

$$\sigma_\nu = \sigma_{\Delta\omega/\omega} = \sqrt{\frac{3\sqrt{3}\rho}{k_u z}} = \rho\sqrt{\frac{18}{N_G}} \approx \sqrt{\frac{0.83\rho}{z/\lambda_u}}, \tag{4.67}$$

where N_G is the number of power gain lengths of evolution.

In the general case, numerical calculation is necessary to obtain these quantities. Figure 4.3 shows the maximum growth rate μ_{Im} and the corresponding coupling parameters g_S and g_A as a function of the energy spread for a Gaussian energy distribution. As expected, the maximum growth rate decreases (and the growth length increases) as a function of σ_η, since electrons with different energies are resonant with different radiation frequencies. This effect for a Gaussian energy spread can be approximated as affecting the gain length via

$$L_G(\sigma_\eta) = \frac{1}{4\rho k_u \mu_{Im}(\sigma_\eta)} \approx L_{G0}\left[1 + (\sigma_\eta/\rho)^2\right], \tag{4.68}$$

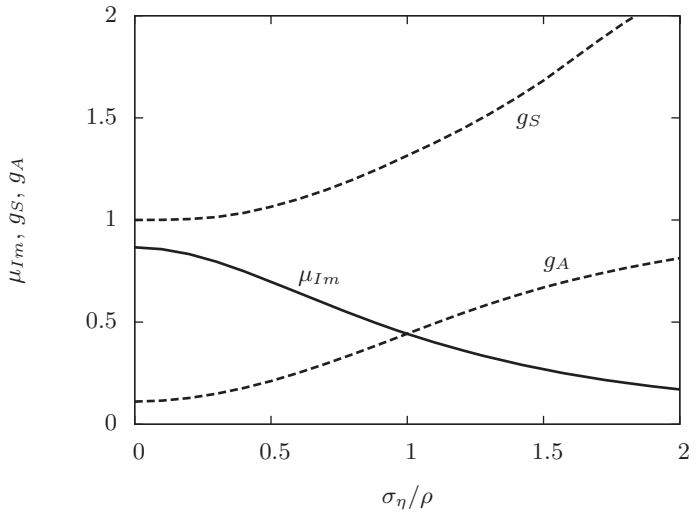

Figure 4.3 Maximum growth rate μ_I, radiation coupling g_A, and shot noise seeding parameter g_S as a function of rms Gaussian energy spread width σ_η.

and we see that the gain length is severely lengthened when when the spread in energies approaches the FEL bandwidth, i.e., when $\sigma_\eta/\rho \gtrsim 1$. Note that the gain length (4.68) is chosen for an optimal detuning $\Delta\nu$, and that the optimal $\Delta\nu$ becomes more negative as σ_η increases.

Additionally, both g_A and g_S are increasing functions of σ_η. The latter g_S gives the relative strength of the shot noise seeded SASE to that produced by any coherent radiation seed, which is an important quantity if one is interested in generating longitudinally coherent FEL light using an external radiation source. As the energy spread increases, one must increase the electromagnetic seed power to overcome the fractional increase in shot noise generated SASE. For small energy spreads $\sigma_\eta \ll \rho$, the quadratic increase in g_S can be ascribed to the energy noise associated with the collective momentum $P(0)$ that we introduced in Sec. 3.4.4.

In the exponential growth regime, Eq. (4.67) implies that the SASE bandwidth decreases as $(\lambda_u/z)^{1/2}$. Hence, during exponential growth the bandwidth decreases more slowly than it does during the spontaneous emission phase where $\Delta\nu \propto \lambda_u/z$. We plot an example illustrating this in Fig. 4.4, where we see that the SASE bandwidth follows that of the undulator radiation for the first few gain lengths, after which it decreases as $(\lambda_u/z)^{1/2}$. The radiation force is set to zero for the simulation of the undulator radiation. Note the difference in bandwidth at saturation $\hat{z} \approx 10$ ($z \sim \lambda_u/\rho$) is a factor of order 2-3, whereas after exponential growth the average SASE power is $\sim 10^5$ to 10^7 times larger than that of simple undulator radiation.

Before saturation, the expression (4.61) can be used to compute the charac-

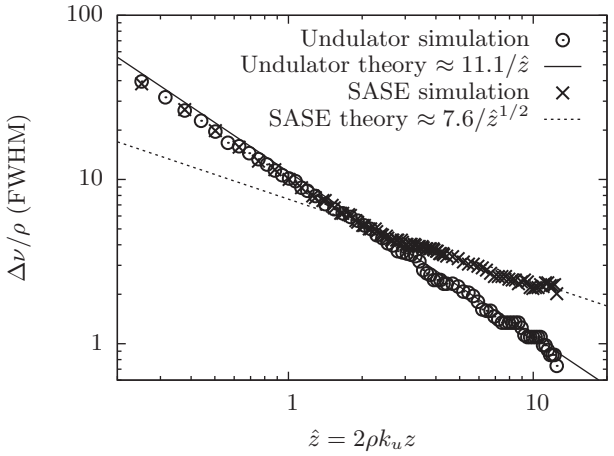

Figure 4.4 Evolution of SASE bandwidth and undulator radiation full-width, half-max (FWHM) bandwidth. The factors 11.1 and 7.6 for the theory lines come from Eqs. (2.72) and (4.67), respectively, using $\rho = 5 \times 10^{-4}$.

teristics of SASE. For example, the coherence time $t_{\rm coh}$ can be computed from the coherence function

$$\mathcal{C}(\tau) \equiv \frac{\left\langle \int dt\ E(t)E^*(t+\tau) \right\rangle}{\left\langle \int dt\ |E(t)|^2 \right\rangle} = \frac{1}{\langle P \rangle} \left\langle \int d\omega\ e^{-i\omega\tau} \frac{dP}{d\omega} \right\rangle, \tag{4.69}$$

where the second line identifies the correlation function with the Fourier transform of the power spectral density using the Weiner-Khinchin theorem. The correlation time $t_{\rm coh} \equiv \int d\tau\ |\mathcal{C}(\tau)|^2$ is easily evaluated using (4.69) and the power spectral density (4.61); the result is quite similar to that of the chaotic light discussed in Sec. 1.2.5, with

$$t_{\rm coh} = \frac{\sqrt{\pi}}{\omega_m \sigma_\nu}. \tag{4.70}$$

Additionally, the quantity $\rho\gamma_r mc^2/2\pi$ in Eq. (4.53) [or (4.61)] may be interpreted as the input noise power contained in the electron beam [4]. The noise power is independent of frequency (white noise), and it can be shown to be equal to the power generated from spontaneous undulator radiation in two power gain lengths [5]. Integrating the SASE term over the frequency, we obtain the electromagnetic power

$$\begin{aligned} P = \int d\omega\ \frac{dP}{d\omega} &= g_S g_A \frac{\rho\,\gamma_r mc^2}{2\pi} \sqrt{2\pi}\omega_1 \sigma_\nu e^{z/L_G} \\ &= g_S g_A \rho P_{\rm beam} \frac{e^{z/L_G}}{\sqrt{2} N_{l_{\rm coh}}}. \end{aligned} \tag{4.71}$$

Here $P_{\rm beam} = (I/e)\gamma_r mc^2$ is the e-beam power and $N_{l_{\rm coh}} = (I/ec)l_{\rm coh}$ is the number of electrons in one coherence length $l_{\rm coh} \equiv ct_{\rm coh} = \lambda_1/(2\sqrt{\pi}\sigma_\nu)$. Since

we expect the saturation power to be about $\rho P_{\rm beam}$, the total amplification factor will be about $N_{l_{\rm coh}}$, which is a large number whose typical magnitude is 10^5 to 10^7.

4.3.3 Temporal fluctuation and correlation of SASE

The SASE radiation consists of a random collection of a large number of coherent pulses, much like synchrotron radiation. To see this in the time domain, we construct the temporal amplitude by Fourier transforming the field in the frequency representation,

$$E_x(z,t) = \int d\nu\; E_\nu(z) e^{i\Delta\nu[(k_1+k_u)z-\omega_1 t]} e^{i(k_1 z-\omega_1 t)}, \tag{4.72}$$

with E_ν given by the growth SASE solution for the case of vanishing energy spread

$$E_\nu(z) = \frac{i\kappa_1 n_e}{2\rho k_u N_\lambda} \frac{e^{-i\mu 2\rho k_u z}}{\mu D'(\mu)} \sum_{j=1}^{N_e} e^{-i\nu\theta_j(0)}. \tag{4.73}$$

In general, the integral cannot be evaluated exactly due to the dependence of μ on $\Delta\nu$. However, in the limit that the energy spread is negligible, an approximate result can be obtained using the second order expansion derived in (4.66). Hence, we insert

$$\mu = -\frac{1}{2}\left[1 - \frac{\Delta\nu}{3\rho} + \frac{(\Delta\nu)^2}{36\rho^2}\right] + i\frac{\sqrt{3}}{2}\left[1 - \frac{(\Delta\nu)^2}{36\rho^2}\right] \tag{4.74}$$

into the exponential of μ, and the resulting expression is a Gaussian integral that can be done analytically. We obtain [6]

$$\begin{aligned} E_x(z,t) \propto \frac{e^{\sqrt{3}\rho k_u z}}{\sqrt{z}} \sum_{j=1}^{N_e} &\exp\left\{-i\omega_1\left[t - \frac{z}{c}(1+\rho\Delta\beta) - t_j\right]\right\} \\ &\times \exp\left\{-\frac{1+i/\sqrt{3}}{4\sigma_\tau^2}\left[t - \frac{z}{c}\left(1+\tfrac{2}{3}\Delta\beta\right) - t_j\right]^2\right\}, \end{aligned} \tag{4.75}$$

where the normalized difference of the average electron beam velocity from unity is $\Delta\beta \equiv 1 - \bar{\beta}_z = (1 + K^2/2)/2\gamma^2$, and the rms temporal width

$$\sigma_\tau = \frac{1}{\sqrt{3}\sigma_\omega} \approx \frac{1}{2\omega_1}\sqrt{\frac{z/\lambda_u}{\rho}}. \tag{4.76}$$

The total field profile (4.75) describes a sum of N_e wave packets of rms pulse length σ_τ that grow exponentially as they propagate. This random collection of modes has the essential properties of chaotic light, although in this case the power grows exponentially with z while its coherence length increases $\sim \sqrt{k_u z}$. Note that the relationship between the rms temporal and spectral widths of these modes differ from the usual $\sigma_\tau\sigma_\omega = 1/2$ due to the quadratic phase dependence in (4.75). We show an example of such temporal evolution of SASE in Fig. 4.5.